Journal of Computational Physics 228 (2009) 3517–3532

Contents lists available at ScienceDirect

Journal of Computational Physics

journal homepage: www.elsevier.com/locate/jcp

Explicit multi-symplectic methods for Klein–Gordon–Schrödinger equations ☆

Jialin Hong [a,*], Shanshan Jiang [b], Chun Li [a]

[a] State Key Laboratory of Scientific and Engineering Computing, Institute of Computational Mathematics and Scientific/Engineering Computing, Academy of Mathematics and System Sciences, Chinese Academy of Sciences, P.O. Box 2719, Beijing 100080, PR China
[b] School of Mathematics Sciences, Peking University, Beijing 100871, PR China

ARTICLE INFO

Article history:
Received 26 March 2007
Received in revised form 4 January 2009
Accepted 5 February 2009
Available online 14 February 2009

Keywords:
Klein–Gordon–Schrödinger equation
Multi-symplectic integrator
Runge–Kutta–Nyström method
Runge–Kutta-type method
Explicit

ABSTRACT

In this paper, we propose explicit multi-symplectic schemes for Klein–Gordon–Schrödinger equation by concatenating suitable symplectic Runge–Kutta-type methods and symplectic Runge–Kutta–Nyström-type methods for discretizing every partial derivative in each sub-equation. It is further shown that methods constructed in this way are multi-symplectic and preserve exactly the discrete charge conservation law provided appropriate boundary conditions. In the aim of the commonly practical applications, a novel 2-order one-parameter family of explicit multi-symplectic schemes through such concatenation is constructed, and the numerous numerical experiments and comparisons are presented to show the efficiency and some advantages of the our newly derived methods. Furthermore, some high-order explicit multi-symplectic schemes of such category are given as well, good performances and efficiencies and some significant advantages for preserving the important invariants are investigated by means of numerical experiments.

1. Introduction

In this paper, we consider the Klein–Gordon–Schrödinger (KGS) equation

$$\begin{cases} i\partial_t \varphi + \frac{1}{2}\partial_{xx}\varphi + u\varphi = 0, & x \in \mathcal{R}, \quad t \geqslant 0, \\ \partial_{tt} u - \partial_{xx} u + u - |\varphi|^2 = 0, & x \in \mathcal{R}, \quad t \geqslant 0, \end{cases} \tag{1.1}$$

which describes a system of conserved scalar nucleons interacting with neutral scalar Mesons coupled with Yukawa interaction, where $\varphi(x,t)$ represents a complex scalar nucleon field, $u(x,t)$ a real scalar meson field, and $i = \sqrt{-1}$. We supplement (1.1) by prescribing the initial-boundary value conditions for $\varphi(x,t)$ and $u(x,t)$ with:

$$\begin{aligned} &\varphi|_{t=0} = \varphi_0(x), \quad u|_{t=0} = u_0(x), \quad u_t|_{t=0} = u_1(x), \\ &\lim_{|x|\to\infty} |\varphi| = 0, \quad \lim_{|x|\to\infty} u = 0, \\ &\lim_{|x|\to\infty} |\partial_x \varphi| = 0, \quad \lim_{|x|\to\infty} \partial_x u = 0, \end{aligned} \tag{1.2}$$

☆ The first author is supported by the Director Innovation Foundation of ICMSEC and AMSS, the Foundation of CAS, the NNSFC (Nos. 19971089, 10371128, 60771054) and the Special Funds for Major State Basic Research Projects of China 2005CB321701.

* Corresponding author.
E-mail addresses: hjl@lsec.cc.ac.cn (J. Hong), jss@math.pku.edu.cn (S. Jiang), lichun@lsec.cc.ac.cn (C. Li).

0021-9991/$ - see front matter © 2009 Elsevier Inc. All rights reserved.
doi:10.1016/j.jcp.2009.02.006

then, we can implement zero (or periodic) boundary conditions on the finite interval for subsequent discretizations and computations. The Eq. (1.1) consists of the classical Schrödinger equation and Klein–Gordon equation. Over the last tens of years, there have been a great deal of work on the numerical solving Schrödinger equations ([9,11] and references therein) and Klein–Gordon equations ([5,14] and references therein). In numerical analysis for ODEs and PDEs, whether or not some special characters or structures of the equations are preserved precisely is an important point in performing reliable numerical integrations, as for this, we refer to it as structure-preserving algorithms. Recently, the multi-symplectic methods, i.e. which preserving multi-symplectic geometric structure under appropriate discretizations, have been proposed and investigated for some important Hamiltonian partial differential equations (HPDEs), such as KdV equation [1], Schrödinger equation [8], Klein–Gordon equation [14] and Dirac equation [7], etc. As for the KGS equation, up to now there have been numerous theoretical results and numerical investigations (see [2,17,12] and references therein). Xiang [17] proposed a conservative spectral method for the periodic initial-value problem for the KGS equation with the nonlinear terms. Bao and Yang [2] suggested a time-splitting pseudo-spectral method for the KGS equation of more general form (the KGS equation we consider in this paper is the standard 1-dimensional KGS equation with some parameters vanished), that is, Fourier pseudo-spectral discretization for the spatial derivatives and Crank–Nicolson/leap-frog schemes for the time derivatives including some technical splitting procedures, and the deduced scheme hence is either explicit or implicit but could be solved explicitly since the KGS equation they considered had the special form in the non-derivative part. Kong et al. [12] first notes that the KGS equation has a natural multi-symplectic structure and proposed the multi-symplectic mid-point scheme for the discretization of the KGS equation, he showed that the multi-symplectic scheme he used preserves the discrete charge conservation law and investigated some important conservative properties numerically as well. Unfortunately, the multi-symplectic mid-point scheme applied to the KGS equation is implicit. It results in a huge expense in numerical solving systems of nonlinear equations at each time step for initial or initial-boundary value problems, especially in the practical applications with 2 or 3 spatial dimensions. Accordingly, it is natural to bring the multi-symplecticity, the intrinsic geometric character of the KGS equation and the explicitness, the computational efficiency and performance together, in other words, to investigate explicit (or as mentioned in Bao et al.[2] "can be solved explicitly") multi-symplectic integrators for the KGS equation.

In [6], authors propose the totally explicit schemes for the model problem – the wave equation. In this paper, the methods are suggested in a different manner, roughly speaking, they are not totally explicit but can be solved explicitly, where also we refer to this as the word explicit, which we will emphasized especially in Section 3. This paper is organized as follows. We outline a multi-symplectic form of the KGS equation (which is a little different from that given in [12]) and briefly discuss some important conservative properties of the equation in the rest of this section. In Section 2, we briefly review the explicit multi-symplectic Runge–Kutta–Nyström methods in the case of Hamiltonian ODEs. In Section 3, we proposed a new class explicit multi-symplectic integrators for KGS equation by using the concatenation of symplectic RK and RKN methods and investigate some discrete properties under the discretization, a new 2-order one-parameter family of schemes is constructed explicitly as an example. We demonstrate some numerical experiments in Section 4, where we use one of the family of schemes we derived in the previous section to simulate the KGS equation and some of its conserved properties, simultaneously, some numerical comparisons with some other explicit 2-order schemes are exhibited. In order to exhibit the good performance and efficiency of our methods, we give an Appendix, in which we construct some high-order schemes and numerical behaviors of them are observed perfectly. The paper ends with conclusions including some of further work.

Set $\varphi(x,t) = q(x,t) + ip(x,t)$, where $p(x,t)$ and $q(x,t)$ are real valued functions, then the Eq. (1.1) can be rewritten as

$$\begin{cases} \partial_t q + \frac{1}{2}\partial_{xx} p + up = 0, \\ \partial_t p - \frac{1}{2}\partial_{xx} q - uq = 0, \\ \partial_{tt} u - \partial_{xx} u + u - (q^2 + p^2) = 0. \end{cases} \tag{1.3}$$

We introduce new variables $g = \partial_x q,\ f = \partial_x p,\ v = \partial_t u,\ w = \partial_x u$. Substituting these into the above system (1.3) and obtain the general form of the multi-symplectic Hamiltonian partial differential equations, which is formulated in the abstract form

$$M\partial_t z + K\partial_x z = \nabla_z S(z), \tag{1.4}$$

where $z = (q,p,g,f,u,v,w)^T$, M and K are two skew-symmetric matrices (which can be singular),

$$M = \begin{pmatrix} 0 & 1 & 0 & 0 & 0 & 0 & 0 \\ -1 & 0 & 0 & 0 & 0 & 0 & 0 \\ 0 & 0 & 0 & 0 & 0 & 0 & 0 \\ 0 & 0 & 0 & 0 & 0 & 0 & 0 \\ 0 & 0 & 0 & 0 & 0 & \frac{1}{2} & 0 \\ 0 & 0 & 0 & 0 & -\frac{1}{2} & 0 & 0 \\ 0 & 0 & 0 & 0 & 0 & 0 & 0 \end{pmatrix}, \quad K = \begin{pmatrix} 0 & 0 & -\frac{1}{2} & 0 & 0 & 0 & 0 \\ 0 & 0 & 0 & -\frac{1}{2} & 0 & 0 & 0 \\ \frac{1}{2} & 0 & 0 & 0 & 0 & 0 & 0 \\ 0 & \frac{1}{2} & 0 & 0 & 0 & 0 & 0 \\ 0 & 0 & 0 & 0 & 0 & 0 & -\frac{1}{2} \\ 0 & 0 & 0 & 0 & 0 & 0 & 0 \\ 0 & 0 & 0 & 0 & \frac{1}{2} & 0 & 0 \end{pmatrix},$$

and $S(z)$ is a real smooth function of the state variable z and for the system (1.1), it is given by

$$S(z) = \frac{1}{2}u(q^2 + p^2) + \frac{1}{4}(g^2 + f^2 - u^2 - v^2 + w^2).$$

The multi-symplectic form for the KGS system formulated in [12] is a little different from that we outlined above. The multi-symplectic Hamiltonian partial differential equation (MHPDEs) (1.4) possesses the multi-symplectic conservation law

$$\partial_t \omega + \partial_x \kappa = 0, \tag{1.5}$$

where

$$\omega = dz \wedge M\,dz, \quad \kappa = dz \wedge K\,dz$$

are differential 2-forms, which presents the geometric character on the phase space, here $\wedge$. stands for the exterior product. After some straightforward calculation, the multi-symplectic conservation law (1.5) for the KGS equations (1.1) can be written in terms of the following equivalent form

$$\partial_t[2dq \wedge dp + du \wedge dv] + \partial_x[dg \wedge dq + df \wedge dp + dw \wedge du] = 0. \tag{1.6}$$

As discussed in many contexts ([3–5,14] and references therein), an arbitrary MHPDEs in the form of Eq. (1.4) has three local conservation laws, i.e. the multi-symplectic conservation law just presented, the energy and momentum conservation laws, which are satisfied where is well defined in the space-time domain. Further, when imposed appropriate boundary conditions, e.g. periodic boundary conditions or zero boundary conditions, one can obtain the three corresponding global conservation laws, by integrating the local ones over the whole spatial domain considered and the flux terms will vanish under the boundary requirements and then the statement is verified. Some important global conservation laws investigated in this paper are listed as follows:

(i) The total energy conservation law

$$\begin{aligned}\mathcal{E}(t) &:= \int_{\mathcal{R}} (u(x,t)^2 + u_t(x,t)^2 + u_x(x,t)^2 + |\varphi_x(x,t)|^2) - 2u(x,t)|\varphi(x,t)|^2\,dx \\ &= \int_{\mathcal{R}} (u(x,0)^2 + u_t(x,0)^2 + u_x(x,0)^2 + |\varphi_x(x,0)|^2) - 2u(x,0)|\varphi(x,0)|^2\,dx := \mathcal{E}(0).\end{aligned} \tag{1.7}$$

(ii) The total momentum conservation law

$$\mathcal{M}(t) := \int_{\mathcal{R}} \mathcal{I}m(\overline{\varphi}(x,t)\varphi_x(x,t)) - u_t(x,t)u_x(x,t)\,dx = \int_{\mathcal{R}} \mathcal{I}m(\overline{\varphi}(x,0)\varphi_x(x,0)) - u_t(x,0)u_x(x,0)\,dx := \mathcal{M}(0), \tag{1.8}$$

where $\mathcal{I}m$ stands for the imaginary part, and $\overline{\varphi}$ denotes the complex conjugate of φ.

(iii) The charge conservation law

$$\mathcal{C}(t) := \int_{\mathcal{R}} |\varphi(x,t)|^2\,dx = \int_{\mathcal{R}} |\varphi_0(x)|^2\,dx := \mathcal{C}(0). \tag{1.9}$$

The former two conservation laws show that the energy and the momentum are conserved all the time in the interacting, and the last one describes the probability of the nucleon particles in the whole space and thus is of course a conserved quantity. We remark here that, corresponds to the three global conservation laws, there exist three local ones, which imply the former under appropriate boundary conditions [8,11].

2. Review of explicit symplectic integrators for Hamiltonian ODEs

As well-known, for the general case of Hamiltonian ODEs, there is **no** symplectic Runge–Kutta (RK) method is explicit. In the separable cases, however, one can find some explicit symplectic schemes, which come mainly from partitioned Runge–Kutta (PRK) methods and Runge–Kutta–Nyström (RKN) methods. For the purpose of this context, we start with the RKN methods applied to the following Hamiltonian dynamical system in the case of ODEs

$$\dot{\mathbf{q}} = \mathbf{M}^{-1}\mathbf{p}, \quad \dot{\mathbf{p}} = -\nabla_{\mathbf{q}} U(\mathbf{q}), \quad \mathbf{p} \times \mathbf{q} \in \mathbb{R}^n \times \mathbb{R}^n, \tag{2.1}$$

where the $\mathbf{q}$ variables represent Lagrangian coordinates, and the $\mathbf{p}$ variables the corresponding momenta. The Hamiltonian of the above system is given by

$$H(\mathbf{p},\mathbf{q}) = \frac{1}{2}\mathbf{p}^T\mathbf{M}^{-1}\mathbf{p} + U(\mathbf{q}),$$

with $\mathbf{M} \in \mathbb{R}^{n\times n}$ being a constant nonsingular and commonly symmetric matrix. It is evident that this system is equivalent to the following second-order differential equations

$$\ddot{\mathbf{q}} = f(\mathbf{q}), \quad f(\mathbf{q}) = -\mathbf{M}^{-1}\nabla_{\mathbf{q}} U(\mathbf{q}). \tag{2.2}$$

Observing the Hamiltonian system (2.1) and its alternative expression (2.2), we can think of it as a first-order differential equation with variables $\mathbf{z} = (\mathbf{p}^T, \mathbf{q}^T)^T$ or with $\mathbf{p}$-variables and $\mathbf{q}$-variables or as a second-order differential system with only $\mathbf{q}$-variables. Different observations may lead to different ideas and then result in different numerical methods here. Precisely saying, it can be discretized by an r-stage RK method in the first case, two r-stage RK methods in the second case, and an r-stage RKN method in the last situation. Furthermore, it is easy to verify that the category of the first discretizations belongs to the second and the second belongs to the last category [15]. But the reverse may not be right. Thus, for the general second-order ODEs (2.2), RKN methods cover both RK and PRK methods and this fact is one of the biggest motivations for us to investigate RKN methods to seek for what we want.

It is known that, an r-stage RKN method, which we denoted by $\mathcal{N}_r = (A, b, c, \beta)$, applied to (2.2) with the local starting point $t = t_k$ yields

$$\begin{aligned} Q_i &= \mathbf{q}_k + c_i h\dot{\mathbf{q}}_k + h^2 \sum_{j=1}^{r} a_{ij} f(Q_j), \\ \mathbf{q}_{k+1} &= \mathbf{q}_k + h\dot{\mathbf{q}}_k + h^2 \sum_{i=1}^{r} \beta_i f(Q_i), \\ \dot{\mathbf{q}}_{k+1} &= \dot{\mathbf{q}}_k + h \sum_{i=1}^{r} b_i f(Q_i), \end{aligned} \tag{2.3}$$

where $\mathbf{q}_k$ denotes an approximation to $\mathbf{q}(t_k)$, $Q_i (i = 1, \ldots, r)$ are the internal stage values, and $\dot{\mathbf{q}}_k$ stands for an approximation to $\dot{\mathbf{q}}(t_k)$. Here, $A = (a_{ij})_{i,j=1}^{r}, b = (b_i)_{i=1}^{r}, c = (c_i)_{i=1}^{r}$ and $\beta = (\beta_i)_{i=1}^{r}$ are the corresponding coefficients of the RKN method. Recalling the symplectic conditions for the RKN methods are given by

$$\beta_i = b_i(1 - c_i), \quad b_i\beta_j - b_i a_{ij} = b_j\beta_i - b_j a_{ji}, \tag{2.4}$$

hence the explicit symplectic RKN method $\mathcal{N}_r$ can be formulated as the form of Butcher's tabular [15]

$$\begin{array}{c|ccccc} c_1 & 0 & 0 & \cdots & 0 & 0 \\ c_2 & b_1(c_2 - c_1) & 0 & \cdots & 0 & 0 \\ c_3 & b_1(c_3 - c_1) & b_2(c_3 - c_2) & \cdots & 0 & 0 \\ \vdots & \vdots & \vdots & \cdots & \vdots & \vdots \\ c_r & b_1(c_r - c_1) & b_2(c_r - c_2) & \ldots & b_{r-1}(c_r - c_{r-1}) & 0 \\ \hline & b_1(1 - c_1) & b_2(1 - c_2) & \cdots & b_{r-1}(1 - c_{r-1}) & b_r(1 - c_r) \\ & b_1 & b_2 & \cdots & b_{r-1} & b_r. \end{array}$$

Then combining with order conditions for various order accuracies, one can get the corresponding explicit symplectic RKN (SRKN) methods of various orders [15].

For an example here, we present a family of 2-stage 2-order explicit SRKN methods with the following Butcher's tabular

$$\begin{array}{c|cc} \frac{1}{2} + \alpha & 0 & 0 \\ \frac{1}{2} + \beta & \beta & 0 \\ \hline & \frac{\beta}{\beta - \alpha}\left(\frac{1}{2} - \alpha\right) & \frac{-\alpha}{\beta - \alpha}\left(\frac{1}{2} - \beta\right) \\ & \frac{\beta}{\beta - \alpha} & \frac{-\alpha}{\beta - \alpha}, \end{array} \tag{2.5}$$

where, α and $\beta, (\alpha \neq \beta)$ are two free parameters. And other higher-order SRKN methods, we refer to [13]. In this paper, we denote the SRKN methods of this class by $\mathcal{SN}_2(\alpha, \beta)$, which plays an important role in the subsequent discussions.

3. Explicit multi-symplectic integrators for Klein–Gordon–Schrödinger equations

In this section, we first construct a novel class of numerical algorithms for the KGS equation by concatenation of various RK-type and RKN-type methods for the numerical approximations to each partial derivative in the KGS equations and then discuss the multi-symplecticity of the newly derived methods. As a practical example, we construct a class of 2-order methods with the scheme (2.5) for the spatial discretization for the KGS equations and discuss the explicitness in details.

For convenience, we reformulate the KGS equations (1.3) into the following ODE expressions in terms of each partial derivative:

In the time direction,

$$\begin{cases} u_t = v, \\ v_t = R, \end{cases} \tag{3.1a}$$

$$\begin{cases} p_t = T, \\ q_t = S, \end{cases} \tag{3.1b}$$

and in the space direction,

$$\begin{cases} u_x = w, \\ w_x = R + u - (q^2 + p^2), \end{cases} \tag{3.2a}$$

$$\begin{cases} p_x = f, \\ f_x = 2(-S - up), \end{cases} \tag{3.2b}$$

$$\begin{cases} q_x = g, \\ g_x = 2(T - uq), \end{cases} \tag{3.2c}$$

where R, S and T are actually functionals of the state variables z. They can also be viewed as symbol variables here, for they only connect the temporal and spatial discretizations together to form fully discrete schemes by eliminating themselves.

We then discretize the above ODEs by using suitable symplectic methods. Applying an r-stage explicit RKN method $\mathcal{N}_r = (A^{(2)}, b^{(2)}, c^{(2)}, \beta)$ to (3.1a), a diagonally implicit RK method $\mathcal{RK}_r = (A^{(1)}, b^{(1)}, c^{(1)})$ to (3.1b), and an s-stage RKN method $\mathcal{N}_s = (\hat{a}, \hat{b}, \hat{c}, \hat{\beta})$ to (3.2a)–(3.2c), then it leads to the following numerical integrator.

In every small local box $[x_0, x_1] \times [t_0, t_1]$ with the starting point (x_0, t_0), we have the following numerical scheme:

$$Q_i^i = q_i^0 + \tau \sum_{j=1}^{i} a_{ij}^{(1)} S_i^j, \tag{3.3}$$

$$q_i^1 = q_i^0 + \tau \sum_{i=1}^{r} b_i^{(1)} S_i^i, \tag{3.4}$$

$$P_i^i = p_i^0 + \tau \sum_{j=1}^{i} a_{ij}^{(1)} T_i^j, \tag{3.5}$$

$$p_i^1 = p_i^0 + \tau \sum_{i=1}^{r} b_i^{(1)} T_i^i, \tag{3.6}$$

$$U_i^i = u_i^0 + c_i^{(2)} \tau v_i^0 + \tau^2 \sum_{j=1}^{i-1} a_{ij}^{(2)} R_i^j, \tag{3.7}$$

$$u_i^1 = u_i^0 + \tau v_i^0 + \tau^2 \sum_{i=1}^{r} \beta_i^{(2)} R_i^i, \tag{3.8}$$

$$v_i^1 = v_i^0 + \tau \sum_{i=1}^{r} b_i^{(2)} R_i^i, \tag{3.9}$$

$$Q_i^i = q_0^i + \hat{c}_i h\, g_0^i + h^2 \sum_{j=1}^{s} \hat{a}_{ij} [2(T_j^i - U_j^i Q_j^i)], \tag{3.10}$$

$$q_1^i = q_0^i + h\, g_0^i + h^2 \sum_{i=1}^{s} \hat{\beta}_i [2(T_i^i - U_i^i Q_i^i)], \tag{3.11}$$

$$g_1^i = g_0^i + h \sum_{i=1}^{s} \hat{b}_i [2(T_i^i - U_i^i Q_i^i)], \tag{3.12}$$

$$P_i^i = p_0^i + \hat{c}_i h\, f_0^i + h^2 \sum_{j=1}^{s} \hat{a}_{ij} [2(-S_j^i - U_j^i P_j^i)], \tag{3.13}$$

$$p_1^i = p_0^i + h\, f_0^i + h^2 \sum_{i=1}^{s} \hat{\beta}_i [2(-S_i^i - U_i^i P_i^i)], \tag{3.14}$$

$$f_1^i = f_0^i + h \sum_{i=1}^{s} \hat{b}_i [2(-S_i^i - U_i^i P_i^i)], \tag{3.15}$$

$$U_i^i = u_0^i + \hat{c}_i h\, w_0^i + h^2 \sum_{j=1}^{s} \hat{a}_{ij} (R_j^i + U_j^i - P_j^{i^2} - Q_j^{i^2}), \tag{3.16}$$

$$u_1^i = u_0^i + h\, w_0^i + h^2 \sum_{i=1}^{s} \hat{\beta}_i (R_i^i + U_i^i - P_i^{i^2} - Q_i^{i^2}), \tag{3.17}$$

$$w_1^i = w_0^i + h \sum_{i=1}^{s} \hat{b}_i (R_i^i + U_i^i - P_i^{i^2} - Q_i^{i^2}). \tag{3.18}$$

Using the corresponding variational equations (we omit here, see [14,7] for details), we obtain the following two equalities,

$$\frac{2dq_i^1\wedge dp_i^1+u_i^1\wedge dv_i^1-2dq_i^0\wedge dp_i^0-du_i^0\wedge dv_i^0}{\tau}=2\tau\sum_{i=1}^{r}b_i^{(1)}[dQ_i^i\wedge dT_i^i+dS_i^i\wedge dP_i^i]+\tau\sum_{i=1}^{r}b_i^{(2)}dU_i^i\wedge dR_i^i, \tag{3.19}$$

and

$$\begin{aligned}&\frac{dg_1^i\wedge dq_1^i+df_1^i\wedge dp_1^i+dw_1^i\wedge du_1^i-dg_0^i\wedge dq_0^i-df_0^i\wedge dp_0^i-dw_0^i\wedge du_0^i}{h}\\&=2h\sum_{\hat{i}=1}^{s}\hat{b}_{\hat{i}}[dT_{\hat{i}}^i\wedge dQ_{\hat{i}}^i+dP_{\hat{i}}^i\wedge dS_{\hat{i}}^i]+h\sum_{\hat{i}=1}^{s}\hat{b}_{\hat{i}}dR_{\hat{i}}^i\wedge dU_{\hat{i}}^i.\end{aligned} \tag{3.20}$$

Then according to the property of wedge product, we have the following theorem:

Theorem 3.1. *With the assumptions that*

$$b_i^{(1)}=b_i^{(2)}=b_i,\quad c_i^{(1)}=c_i^{(2)}=c_i,\qquad 1\leqslant i\leqslant r, \tag{3.21}$$

the method (3.3)–(3.18) is multi-symplectic and satisfies the discrete multi-symplectic conservation law

$$\begin{aligned}&\tau\sum_{i=1}^{r}b_i[dg_1^i\wedge dq_1^i+df_1^i\wedge dp_1^i+dw_1^i\wedge du_1^i-dg_0^i\wedge dq_0^i-df_0^i\wedge dp_0^i-dw_0^i\wedge du_0^i]\\&+h\sum_{\hat{i}=1}^{s}\hat{b}_{\hat{i}}[2dq_i^1\wedge dp_i^1+du_{k,\hat{i}}^1\wedge dv_i^1-2dq_i^0\wedge dp_i^0-du_{k,i}^0\wedge dv_i^0]=0,\end{aligned} \tag{3.22}$$

if it obeys the symplectic conditions:

$$b_i^{(1)}b_j^{(1)}-b_i^{(1)}a_{ij}^{(1)}-b_j^{(1)}a_{ji}^{(1)}=0, \tag{3.23}$$

$$\beta_i^{(2)}=b_i^{(2)}(1-c_i^{(2)}),\quad b_i^{(2)}\beta_j^{(2)}-b_i^{(2)}a_{ij}^{(2)}=b_j^{(2)}\beta_i^{(2)}-b_j^{(2)}a_{ji}^{(2)}, \tag{3.24}$$

$$\hat{\beta}_{\hat{i}}=\hat{b}_{\hat{i}}(1-\hat{c}_{\hat{i}}),\quad \hat{b}_{\hat{i}}\hat{\beta}_{\hat{j}}-\hat{b}_{\hat{i}}\hat{a}_{\hat{i}\hat{j}}=\hat{b}_{\hat{j}}\hat{\beta}_{\hat{i}}-\hat{b}_{\hat{j}}\hat{a}_{\hat{j}\hat{i}}, \tag{3.25}$$

for all $\hat{i},\hat{j}=1,\ldots,s$, *and* $i,j=1,\ldots,r$.

The proof is similar with some existing references [14,8] and is thus omitted here.

As discussed in [7], we have a discrete analogue of the charge conservation law (1.9) under the numerical discretizations presented in (3.3)–(3.18).

Theorem 3.2. *If the method (3.3)–(3.18) satisfies the following symplectic conditions*

$$b_i^{(1)}b_j^{(1)}-b_i^{(1)}a_{ij}^{(1)}-b_j^{(1)}a_{ji}^{(1)}=0, \tag{3.26}$$

$$\hat{\beta}_{\hat{i}}=\hat{b}_{\hat{i}}(1-\hat{c}_{\hat{i}}),\quad \hat{b}_{\hat{i}}\hat{\beta}_{\hat{j}}-\hat{b}_{\hat{i}}\hat{a}_{\hat{i}\hat{j}}=\hat{b}_{\hat{j}}\hat{\beta}_{\hat{i}}-\hat{b}_{\hat{j}}\hat{a}_{\hat{j}\hat{i}}, \tag{3.27}$$

for all $\hat{i},\hat{j}=1,\ldots,s$, *and* $i,j=1,\ldots,r$, *then it gives rise to the following discrete charge conservation law*

$$h\sum_{k}\sum_{\hat{i}=1}^{s}\hat{b}_{\hat{i}}|\varphi_{k,\hat{i}}^{l+1}|^2=h\sum_{k}\sum_{\hat{i}=1}^{s}\hat{b}_{\hat{i}}|\varphi_{k,\hat{i}}^{l}|^2, \tag{3.28}$$

provided with zero boundary conditions, i.e. $\varphi_0^l=\varphi_J^l=0,\forall\, l$.

Note that the assumptions imposed in Theorem 3.2 are weaker than that in Theorem 3.1. In order to discuss the explicitness of the multi-symplectic methods constructed here, we start with a class of low-order ones as a reference model.

First, we apply a family of explicit SRKN methods $\mathcal{SN}_2(\alpha,\frac{1}{2}+\alpha)$

$$\begin{array}{c|cc}\frac{1}{2}+\alpha & 0 & 0\\ 1+\alpha & \frac{1}{2}+\alpha & 0\\ \hline & \frac{1}{2}-2\alpha^2 & 2\alpha^2\\ & 1+2\alpha & -2\alpha\end{array}, \tag{3.29}$$

which belongs to the class $\mathcal{SN}_2(\alpha,\beta)$ with $\beta=\frac{1}{2}+\alpha$ to (3.1a). Now, a new problem arises: Does there exist a diagonally implicit 2-stage 2-order RK method $\mathcal{RK}_r=(A^{(1)},b^{(1)},c^{(1)})$ with the requirements $(c_1^{(1)},c_2^{(1)})=(\frac{1}{2}+\alpha,1+\alpha)$ and $(b_1^{(1)},b_2^{(1)})=(1+2\alpha,-2\alpha)$ that are imposed in Theorem 3.1 for multi-symplecticity? It is referred to as consistent diagonally implicit RK methods throughout this paper. Fortunately, the following diagonally implicit SRK method, which is denoted by $\mathcal{SR}_2(\alpha)$

$$\begin{array}{c|cc}\frac{1}{2}+\alpha & \frac{1}{2}+\alpha & 0\\ 1+\alpha & 1+2\alpha & -\alpha\\ \hline & 1+2\alpha & -2\alpha\end{array}, \tag{3.30}$$

satisfies the conditions. Now we apply $\mathcal{SR}_2(\alpha)$ to (3.1b). Then the schemes for time discretizations are available, as for the space, we make use of the explicit SRKN method denoted by $\mathcal{SN}_2(-\frac{1}{2},\frac{1}{2})$ [15]

$$\begin{array}{c|cc} 0 & 0 & 0 \\ 1 & \frac{1}{2} & 0 \\ \hline & \frac{1}{2} & 0 \\ & \frac{1}{2} & \frac{1}{2} \end{array} \tag{3.31}$$

to approximate the second-order derivatives in (3.2a)–(3.2c). And such discretization is multi-symplectic, according to Theorems 3.1 and 3.2. *Note that in space direction, we can also make use of implicit RKN methods which would not affect the so-called explicitness of the whole scheme.*

Corresponds to the method (3.3)–(3.18), applying the schemes (3.29)–(3.31) to the KGS equation (1.3) as stated above yields that

$$\begin{aligned}
&\varphi_k^{l+\frac{1}{2}+\alpha} = \varphi_k^l + \left(\frac{1}{2}+\alpha\right)\tau Y_k^{l+\frac{1}{2}+\alpha},\\
&\varphi_k^{l+1+\alpha} = \varphi_k^l + (1+2\alpha)\tau Y_k^{l+\frac{1}{2}+\alpha} + (-\alpha)\tau Y_k^{l+1+\alpha},\\
&\varphi_k^{l+1} = \varphi_k^l + (1+2\alpha)\tau Y_k^{l+\frac{1}{2}+\alpha} + (-2\alpha)\tau Y_k^{l+1+\alpha},\\
&\varphi_{k+1}^i = \varphi_k^i + h\phi_k^i + \frac{1}{2}h^2(-2iY_k^i - 2u_k^i\varphi_k^i), \quad i = l+\frac{1}{2}+\alpha, l+1+\alpha,\\
&\phi_{k+1}^i = \phi_{k+1}^i + \frac{1}{2}h(-2iY_k^i - 2u_k^i\varphi_k^i) + \frac{1}{2}h(-2iY_{k+1}^i - 2u_{k+1}^i\varphi_{k+1}^i), \quad i = l+\frac{1}{2}+\alpha, l+1+\alpha,\\
&u_k^{l+\frac{1}{2}+\alpha} = u_k^l + \left(\frac{1}{2}+\alpha\right)\tau v_k^l,\\
&u_k^{l+1+\alpha} = u_k^l + (1+\alpha)\tau v_k^l + (\frac{1}{2}+\alpha)\tau^2 R_k^{l+\frac{1}{2}+\alpha},\\
&u_k^{l+1} = u_k^l + \tau v_k^l + \left(\frac{1}{2}-2\alpha^2\right)\tau^2 R_k^{l+\frac{1}{2}+\alpha} + (2\alpha^2)\tau^2 R_k^{l+1+\alpha},\\
&v_k^{l+1} = v_k^l + (1+2\alpha)\tau R_k^{l+\frac{1}{2}+\alpha} + (-2\alpha)\tau R_k^{l+1+\alpha},\\
&u_{k+1}^i = u_k^i + hw_k^i + \frac{1}{2}h^2(R_k^i + u_k^i - |\varphi_k^i|^2), \quad i = l+\frac{1}{2}+\alpha, l+1+\alpha,\\
&w_{k+1}^i = w_{k+1}^i + \frac{1}{2}h(R_k^i + u_k^i - |\varphi_k^i|^2) + \frac{1}{2}h(R_{k+1}^i + u_{k+1}^i - |\varphi_{k+1}^i|^2), \quad i = l+\frac{1}{2}+\alpha, l+1+\alpha,
\end{aligned}$$

where $Y = S + iT$, ϕ approximates φ_x, the local box becomes $[x_k, x_{k+1}] \times [t_l, t_{l+1}]$, and l and k are non-negative integers.

Eliminating the symbol variables Y, R and the introduced variables ϕ, v, w, the numerical scheme is rewritten as follows:

$$\varphi_k^{l+\frac{1}{2}+\alpha} = \varphi_k^l + \left(\frac{1}{2}+\alpha\right)\tau i\left[\frac{\varphi_{k+1}^{l+\frac{1}{2}+\alpha} - 2\varphi_k^{l+\frac{1}{2}+\alpha} + \varphi_{k-1}^{l+\frac{1}{2}+\alpha}}{2h^2} + u_k^{l+\frac{1}{2}+\alpha}\varphi_k^{l+\frac{1}{2}+\alpha}\right], \tag{3.32}$$

$$\begin{aligned}
\varphi_k^{l+1+\alpha} = \varphi_k^l &+ (1+2\alpha)\tau i\left[\frac{\varphi_{k+1}^{l+\frac{1}{2}+\alpha} - 2\varphi_k^{l+\frac{1}{2}+\alpha} + \varphi_{k-1}^{l+\frac{1}{2}+\alpha}}{2h^2} + u_k^{l+\frac{1}{2}+\alpha}\varphi_k^{l+\frac{1}{2}+\alpha}\right]\\
&- \alpha\tau i\left[\frac{\varphi_{k+1}^{l+1+\alpha} - 2\varphi_k^{l+1+\alpha} + \varphi_{k-1}^{l+1+\alpha}}{2h^2} + u_k^{l+1+\alpha}\varphi_k^{l+1+\alpha}\right],
\end{aligned} \tag{3.33}$$

$$\begin{aligned}
\varphi_k^{l+1} = \varphi_k^l &+ (1+2\alpha)\tau i\left[\frac{\varphi_{k+1}^{l+\frac{1}{2}+\alpha} - 2\varphi_k^{l+\frac{1}{2}+\alpha} + \varphi_{k-1}^{l+\frac{1}{2}+\alpha}}{2h^2} + u_k^{l+\frac{1}{2}+\alpha}\varphi_k^{l+\frac{1}{2}+\alpha}\right]\\
&- 2\alpha\tau i\left[\frac{\varphi_{k+1}^{l+1+\alpha} - 2\varphi_k^{l+1+\alpha} + \varphi_{k-1}^{l+1+\alpha}}{2h^2} + u_k^{l+1+\alpha}\varphi_k^{l+1+\alpha}\right],
\end{aligned} \tag{3.34}$$

$$u_k^{l+\frac{1}{2}+\alpha} = u_k^l + \left(\frac{1}{2}+\alpha\right)\tau v_k^l, \tag{3.35}$$

$$u_k^{l+1+\alpha} = u_k^l + (1+\alpha)\tau v_k^l + \left(\frac{1}{2}+\alpha\right)\tau^2\left[\frac{u_{k+1}^{l+\frac{1}{2}+\alpha} - 2u_k^{l+\frac{1}{2}+\alpha} + u_{k-1}^{l+\frac{1}{2}+\alpha}}{h^2} - u_k^{l+\frac{1}{2}+\alpha} + |\varphi_k^{l+\frac{1}{2}+\alpha}|^2\right], \tag{3.36}$$

$$u_k^{l+1} = u_k^l + \tau v_k^l + \left(\frac{1}{2} - 2\alpha^2\right)\tau^2 \left[\frac{u_{k+1}^{l+\frac{1}{2}+\alpha} - 2u_k^{l+\frac{1}{2}+\alpha} + u_{k-1}^{l+\frac{1}{2}+\alpha}}{h^2} - u_k^{l+\frac{1}{2}+\alpha} + |\varphi_k^{l+\frac{1}{2}+\alpha}|^2\right] + 2\alpha^2\tau^2 \left[\frac{u_{k+1}^{l+1+\alpha} - 2u_k^{l+1+\alpha} + u_{k-1}^{l+1+\alpha}}{h^2} - u_k^{l+1+\alpha} + |\varphi_k^{l+1+\alpha}|^2\right], \tag{3.37}$$

$$v_k^{l+1} = v_k^l + (1+2\alpha)\tau \left[\frac{u_{k+1}^{l+\frac{1}{2}+\alpha} - 2u_k^{l+\frac{1}{2}+\alpha} + u_{k-1}^{l+\frac{1}{2}+\alpha}}{h^2} - u_k^{l+\frac{1}{2}+\alpha} + |\varphi_k^{l+\frac{1}{2}+\alpha}|^2\right] - 2\alpha\tau \left[\frac{u_{k+1}^{l+1+\alpha} - 2u_k^{l+1+\alpha} + u_{k-1}^{l+1+\alpha}}{h^2} - u_k^{l+1+\alpha} + |\varphi_k^{l+1+\alpha}|^2\right]. \tag{3.38}$$

We refer to the above numerical scheme as SRNN$_2(\alpha)$, which we can see is of order 2 in both space and time, and it gives rise to one-parameter family of multi-symplectic integrators for (1.1).

Proposition 3.3. *The numerical scheme SRNN$_2(\alpha)$ is multi-symplectic, and it preserves the following discrete charge conservation law*

$$\frac{1}{2}h\sum_k |\varphi_k^{l+1}|^2 + \frac{1}{2}h\sum_k |\varphi_{k+1}^{l+1}|^2 = \frac{1}{2}h\sum_k |\varphi_k^l|^2 + \frac{1}{2}h\sum_k |\varphi_{k+1}^l|^2,$$

provided with zero boundary conditions, i.e. $\varphi_0^l = \varphi_J^l = 0, \forall\ l$.

Moreover, SRNN$_2(\alpha)$ advances explicitly from (φ_k^l, u_k^l) to $(\varphi_k^{l+1}, u_k^{l+1})$ without any iterative process, which can be verified by employing the following algorithm:

step1. Initial value u_k^0, and $v_k^0 \overset{(3.35)}{\rightarrow} u_k^{\frac{1}{2}+\alpha}$;
step2. $u_k^{\frac{1}{2}+\alpha}$, andinitialvalue $\varphi_k^0 \overset{(3.32)}{\rightarrow} \varphi_k^{\frac{1}{2}+\alpha}$;
step3. $u_k^{\frac{1}{2}+\alpha}, \varphi_k^{\frac{1}{2}+\alpha}$andinitialvalue $u_k^0, v_k^0 \overset{(3.36)}{\rightarrow} u_k^{1+\alpha}$;
step4. $u_k^{\frac{1}{2}+\alpha}, u_k^{1+\alpha}, \varphi_k^{\frac{1}{2}+\alpha}$ and initial value $\varphi_k^0 \overset{(3.33)}{\rightarrow} \varphi_k^{1+\alpha}$;
step5. $u_k^{\frac{1}{2}+\alpha}, u_k^{1+\alpha}, \varphi_k^{\frac{1}{2}+\alpha}, \varphi_k^{1+\alpha}$ and initial value $\varphi_k^0, u_k^0, v_k^0 \overset{(3.34),(3.37),(3.38)}{\rightarrow} \varphi_k^1, u_k^1, v_k^1$;
step6. $\varphi_k^0 = \varphi_k^1, u_k^0 = u_k^1, v_k^0 = v_k^1$, return to step1, and continue running.

The key point for the explicitness in the above manipulation depends on the special character of the KGS equations, the first equation in the system (1.1) is linear with respect to variable φ and this is well inherited by the discretizations (3.32)–(3.34). More concretely, if the values of u-variables are known in the nonlinear term $u\varphi$, we can obtain the unknown numerical values of φ-variables by solving a linear system.

It should be emphasized here that *we say numerical methods for solving the system (1.1) explicitly means that advancing from* (φ_k^l, u_k^l) *to* $(\varphi_k^{l+1}, u_k^{l+1})$ *without any iterative process, i.e. avoid solving any nonlinear equation at each time level.* The four schemes listed later are all called "explicit" method in this sense.

A good way maybe the best way to study a numerical method for a present model is to perform its investigations in computers. We will whereafter make some actual numerical experiments by using the method SRNN$_2(\alpha)$ we just constructed. In order to do numerical comparisons, we provide three other 2-order explicit methods, along with SRNN$_2(\alpha)$ are referred to as schemes I, II, III & IV and listed as follows:

i. Scheme I is the conservative scheme

$$i\frac{\varphi_k^{l+1} - \varphi_k^l}{\tau} + \frac{1}{4}\left[\frac{\varphi_{k+1}^{l+1} - 2\varphi_k^{l+1} + \varphi_{k-1}^{l+1}}{h^2} + \frac{\varphi_{k+1}^l - 2\varphi_k^l + \varphi_{k-1}^l}{h^2}\right] + \frac{1}{4}(u_k^l + u_k^{l+1})(\varphi_k^l + \varphi_k^{l+1}) = 0,$$

$$\frac{u_k^{l+1} - 2u_k^l + u_k^{l-1}}{\tau^2} - \frac{u_{k+1}^l - 2u_k^l + u_{k-1}^l}{h^2} + \frac{1}{2}(u_k^{l+1} + u_k^{l-1}) - |\varphi_k^l|^2 = 0.$$

We remark here that scheme I preserves both the discrete charge conservation law and the discrete total energy law exactly, more details referred to Zhang [18].

ii. Scheme II

$$i\frac{\varphi_k^{l+1} - \varphi_k^l}{\tau} + \frac{1}{4}\left[\frac{\varphi_{k+1}^{l+1} - 2\varphi_k^{l+1} + \varphi_{k-1}^{l+1}}{h^2} + \frac{\varphi_{k+1}^l - 2\varphi_k^l + \varphi_{k-1}^l}{h^2}\right] + \frac{1}{4}(u_k^l + u_k^{l+1})(\varphi_k^l + \varphi_k^{l+1}) = 0,$$

$$\frac{u_k^{l+1} - 2u_k^l + u_k^{l-1}}{\tau^2} - \frac{u_{k+1}^l - 2u_k^l + u_{k-1}^l}{h^2} + u_k^l - |\varphi_k^l|^2 = 0,$$

is a widely used scheme, which is obtained by applying the modified Crank–Nicolson scheme to the first equation in (1.1), and the five-point scheme to the second equation.

iii. Scheme III is given by

$$i\frac{\varphi_k^{l+1}-\varphi_k^l}{\tau}+\frac{1}{4}\left[\frac{\varphi_{k+1}^{l+1}-2\varphi_k^{l+1}+\varphi_{k-1}^{l+1}}{h^2}+\frac{\varphi_{k+1}^{l}-2\varphi_k^{l}+\varphi_{k-1}^{l}}{h^2}\right]+\frac{1}{2}(u_k^l+\frac{1}{2}\tau v_k^l)(\varphi_k^l+\varphi_k^{l+1})=0,$$

$$u_k^{l+1}=u_k^l+\tau v_k^l+\frac{1}{2}\tau^2\left[\frac{u_{k+1}^l-2u_k^l+u_{k-1}^l}{h^2}-u_k^l+|\varphi_k^l|^2\right],$$

$$v_k^{l+1}=v_k^l+\tau\left[\frac{u_{k+1}^l-2u_k^l+u_{k-1}^l}{h^2}+\frac{1}{2}\tau\frac{v_{k+1}^l-2v_k^l+v_{k-1}^l}{h^2}-u_k^l-\frac{1}{2}\tau v_k^l+\frac{1}{4}|\varphi_k^l+\varphi_k^{l+1}|^2\right].$$

This is a non-multi-symplectic method.

iv. Scheme IV is the multi-symplectic scheme $\mathrm{SRNN}_2(\alpha)$, which we have constructed.

We give some remarks for the four schemes here. First, they are all explicit, this is an important precondition we should conform in numerical comparisons. It is unfair to carry out comparisons between explicit methods and implicit methods over long-time simulation, since the implicit schemes, in general, have better stabilities. Second, they are of 2 order, i.e. the truncation errors are all in the order of $\mathcal{O}(h^2+\tau^2)$; it is the basis for us to compare the magnitudes of various errors by using the four schemes. Moreover, they are conditionally linearly stable (by using the standard Von Neumann analysis), on this point, we refer to [6,10]. Last, they all preserve their corresponding discrete analogues of the charge conservation law exactly.

The results of the numerical experiments are presented in the following section, all numerical comparisons presented among the four schemes are processed under the same numerical conditions.

4. Numerical experiments

Consider the following solitary-wave solutions of system (1.1)

$$\begin{aligned}\varphi(x,t,q)&=\frac{3\sqrt{2}}{4\sqrt{1-q^2}}\operatorname{sech}^2\frac{1}{2\sqrt{1-q^2}}(x-qt)\exp\left(i\left(qx+\frac{1-q^2+q^4}{2(1-q^2)}t\right)\right),\\ u(x,t,q)&=\frac{3}{4(1-q^2)}\operatorname{sech}^2\frac{1}{2\sqrt{1-q^2}}(x-qt),\end{aligned}\tag{4.1}$$

where, $0\leqslant|q|\leqslant 1$ indicates the propagating velocity of wave. In our numerical trials, we take the following initial conditions

$$\varphi_0(x)=\varphi(x,0,q)\quad u_0(x)=u(x,0,q),\quad v_0(x)=u_t(x,t,q)|_{t=0},$$

which are evidently obtained from the exact solutions (4.1) by setting $t=0$.

Observing that the analytic solutions in (4.1) are exponentially decreasing when $|x|$ tends to infinity for any fixing t and noting that our numerical computations must be implemented on a finite spatial interval, we take zero boundary conditions over the space domain $[-L,L]$ with $L=40$, namely

$$\varphi(-L,t)=\varphi(L,t)=0,\quad u(-L,t)=u(L,t)=0,\quad u_t(-L,t)=u_t(L,t)=0.$$

Next, we define $\mathcal{E}_L^l$ as the discrete form of total energy (1.7) at time-step t_l to approximate the continuous total energy $\mathcal{E}(t_l)$, and

$$(\mathcal{E}_{te})_l=\mathcal{E}_L^l-\mathcal{E}_L^0,\tag{4.2}$$

denotes the global error propagation of total energy, and $\mathcal{M}_L^l$ as the discrete form of total momentum (1.8), and $(\mathcal{E}_{tm})_l=\mathcal{M}_L^l-\mathcal{M}_L^0$ as the corresponding global error propagation. Further, we set

$$(\mathrm{error}_\varphi)_l=\max_k|\varphi(x_k,t_l)-\varphi_k^l|,\quad(\mathrm{error}_u)_l=\max_k|u(x_k,t_l)-u_k^l|\tag{4.3}$$

to stand for the maximum errors of solutions at the time-step t_l. Here, $\varphi(x_k,t_l)$ and φ_k^l are value of the exact solution and numerical solution at (x_k,t_l), respectively, so do $u(x_k,t_l)$ and u_k^l. As stated in Theorem 3.2, we use

$$\mathcal{C}_L^l=h\sum_k\sum_{\hat{i}=1}^{s}\hat{b}_{\hat{i}}|\varphi_{k,\hat{i}}^l|^2\tag{4.4}$$

to represent the discrete charge conservation law, and

$$(\mathcal{E}_{tc})_l=\mathcal{C}_L^l-\mathcal{C}_L^0$$

the global error of the discrete charge conservation law.

In Figs. 1–4, we exhibit maximum errors of numerical solutions, global errors of charge conservation law, total energy and total momentum over long time interval $[0, 80]$ for $q = 0.1$, with the space step $h = 0.1$ and the time step $\tau = 0.01$ for schemes (I–IV).

Fig. 1 presents both the maximum errors of solutions $\varphi(x,t)$ (above) and $u(x,t)$ (below). The maximum errors of $\varphi(x,t)$ all grow like a linear line with very small local oscillations almost unobservable in the present scale of the plot (Left) and moreover, the four curves displayed in left-top plot of Fig. 1 are almost the same and we almost can't distinguish from one to another. Only when viewed from the partial enlarged detail (right), we can see some differences; The errors of $u(x,t)$ also exhibited the similar behaviors. Anyway, we can say that the errors display in this figure behave all normally and reasonably.

The global errors in preserving the discrete charge conservation laws are exhibited in Fig. 2 with different line types. It shows that all the four schemes preserve their corresponding discrete analogues of the charge conservation law perfectly, in the sense of roundoff along so long time $[0, 80]$. Comparing with the former three schemes, we find that the error obtained by using Scheme IV behaves a little better, that is, there is fewer error accumulations than the others.

Figs. 3 and 4 show the global errors in preserving the discrete analogues of the discrete total energy and momentum, respectively. Other than the special conservative schemes, e.g. the energy/momentum-preserving algorithms, the majority of numerical methods, involving the symplectic and multi-symplectic methods, cannot preserve energy and momentum in nonlinear cases in general. Observing from the 4 graphs in Fig. 3, one see that only scheme I preserves the discrete energy in the magnitude within roundoff, it is not a surprise that this scheme is an energy-preserving scheme [18], but it brings slight error accumulations with the evolution of time. As for schemes II and III, however, it is not so satisfactory for both of them in preserving the discrete total energy. Observing from the right-top plot in Fig. 3, the error by using scheme II oscillates more and more rapidly and the amplitude of the oscillation grows bigger and bigger, this can be called instability to some extent; the numerical result in the left-below graph in Fig. 3 grows linearly, and it shows that a linear instability

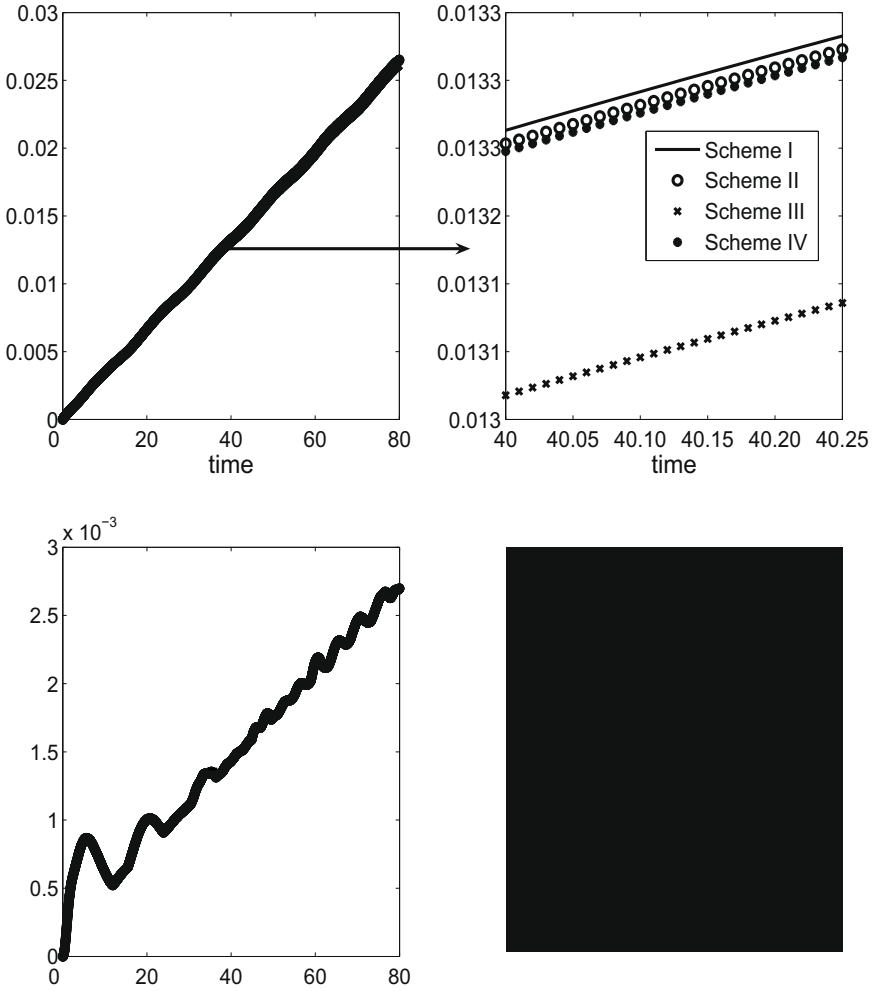

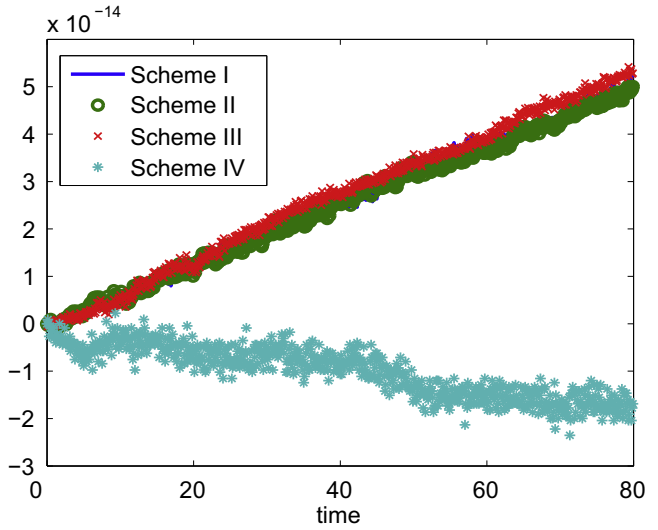

Fig. 2. Maximum error of charge conservation law $(\mathcal{E}_{tc})_l$ as a function of the time-step t_l for different schemes.

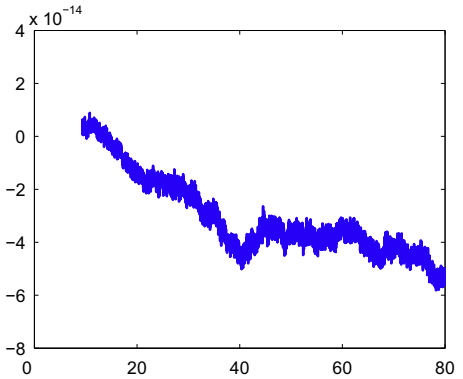

for scheme III in preserving the total energy. Now pay attention to the fourth graph in this figure, the error presented here is obtained by scheme IV and we find that it oscillates reasonably and equably within a small interval near 0 in the scale of $\mathcal{O}(10^{-9})$ all the time, and the amplitude of the oscillation almost does not change over so long time. Then we conclude that scheme IV has a good stability with respect to the total energy conservation law though it can't preserve the energy pre-

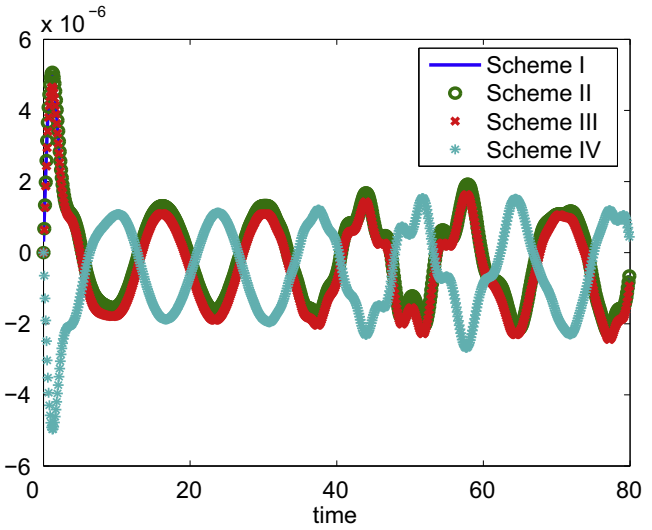

Fig. 4. Global error of total momentum $(\mathcal{E}_{tm})_l$ as a function of the time-step t_l for different schemes.

cisely. Fig. 4 show that all the four schemes preserve the discrete total momentum in the scale of $\mathcal{O}(10^{-6})$ and stay stable. It is a surprise to us that the errors in momentum by the four schemes are almost the same.

According to the numerical results displayed in the previous four figures, with the comparisons and analysis given above, we conclude that the multi-symplectic schemes we presented have not only good performance and efficiency, the perfect preserving in the discrete charge conservation law and the stable behaviors in preserving the discrete momentum and energy conservation laws as well as sometimes a little better than the other three schemes, but also an exact preservation of the multi-symplectic geometric structure in phase space.

5. Conclusions

In this paper, we concatenate the ideas of multi-symplectic integrators (first considered in [12]) and the explicit numerical schemes (first proposed and emphasized in [2]) for KGS equation. And a novel class of explicit multi-symplectic integrators for the 1-dimensional KGS equation is presented and investigated. Moreover, a corresponding discrete charge conservation law is obtained under the multi-symplectic discretizations. The low-order and high-order (in the following Appendix) multi-symplectic schemes demonstrate well in the numerical investigations, they show not only the good performance and efficiency, but also the perfect numerical behaviors; i.e. the charge is conserved within roundoff, and it is known that, in general, multi-symplectic methods can not preserve the energy and momentum exactly, but the numerical results show that the methods utilized preserve the energy and momentum very sharply. In numerical solving KGS equation, to avoid huge numerical cost in using various iterative methods for solving nonlinear algebraic systems at each time step, the idea of explicitness of numerical schemes in this paper could be introduced into studying high-dimensional (e.g. 2 or 3-dimensional) KGS equations. In numerical experiments we also meet some unsolved theoretical problems, for example, the two conjectures in the end of the following Appendix. The study of explicit multi-symplectic methods for KGS equations is just at the beginning.

Appendix. High-order explicit multi-symplectic integrators

Reich [14] carried out 2-stage 4-order Gauss–Legendre collocation RK method in the numerical experiments. Wang and Wang [16] proposed high-order multi-symplectic methods through by the compositions of some existing low-order schemes. To investigate numerically the performance and efficiency of the high-order multi-symplectic methods should be important and interesting. Now we pay attention to the numerical implementation of the high-order multi-symplectic methods.

Firstly, we apply a high-order explicit symplectic RKN (SRKN) method of order 4 and stage 3

$$\begin{array}{c|ccc} \frac{1}{2}-a & 0 & 0 & 0 \\ \frac{1}{2} & \frac{1}{24a} & 0 & 0 \\ \frac{1}{2}+a & \frac{1}{12a} & (1-\frac{1}{12a^2})a & 0 \\ \hline & \frac{1}{24a^2}(\frac{1}{2}+a) & \frac{1}{2}(1-\frac{1}{12a^2}) & \frac{1}{24a^2}(\frac{1}{2}-a) \\ & \frac{1}{24a^2} & 1-\frac{1}{12a^2} & \frac{1}{24a^2} \end{array} \tag{5.5}$$

in the t-direction to the second equation of the KGS system (1.1) and a consistent diagonally implicit SRK method of order 4

$$\begin{array}{c|ccc} \frac{1}{2}-a & \frac{1}{48a^2} & 0 & 0 \\ \frac{1}{2} & \frac{1}{24a^2} & \frac{1}{2}-\frac{1}{24a^2} & 0 \\ \frac{1}{2}+a & \frac{1}{24a^2} & 1-\frac{1}{12a^2} & \frac{1}{48a^2} \\ \hline & \frac{1}{24a^2} & 1-\frac{1}{12a^2} & \frac{1}{24a^2} \end{array} \tag{5.6}$$

in the t-direction to the first equation, where, a is the real root of $48x^3 - 24x^2 + 1$. With regard to the spatial discretizations, we apply $\mathcal{SN}_2(-\frac{1}{2},\frac{1}{2})$ to both the equations in the KGS equations (1.1). Then, we get another explicit multi-symplectic scheme denoted by $\mathcal{SN}_{42}$, which is of high-order in time direction.

Secondly, we apply the schemes $\mathcal{SR}_2(\alpha)$ and $\mathcal{SN}_2(\alpha,\frac{1}{2}+\alpha)$ with both take $\alpha=\frac{1}{6}$ to the first and second equations in (1.1) respectively for time discretizations and a consistent high-order implicit symplectic RKN method of order 4 and stage 3

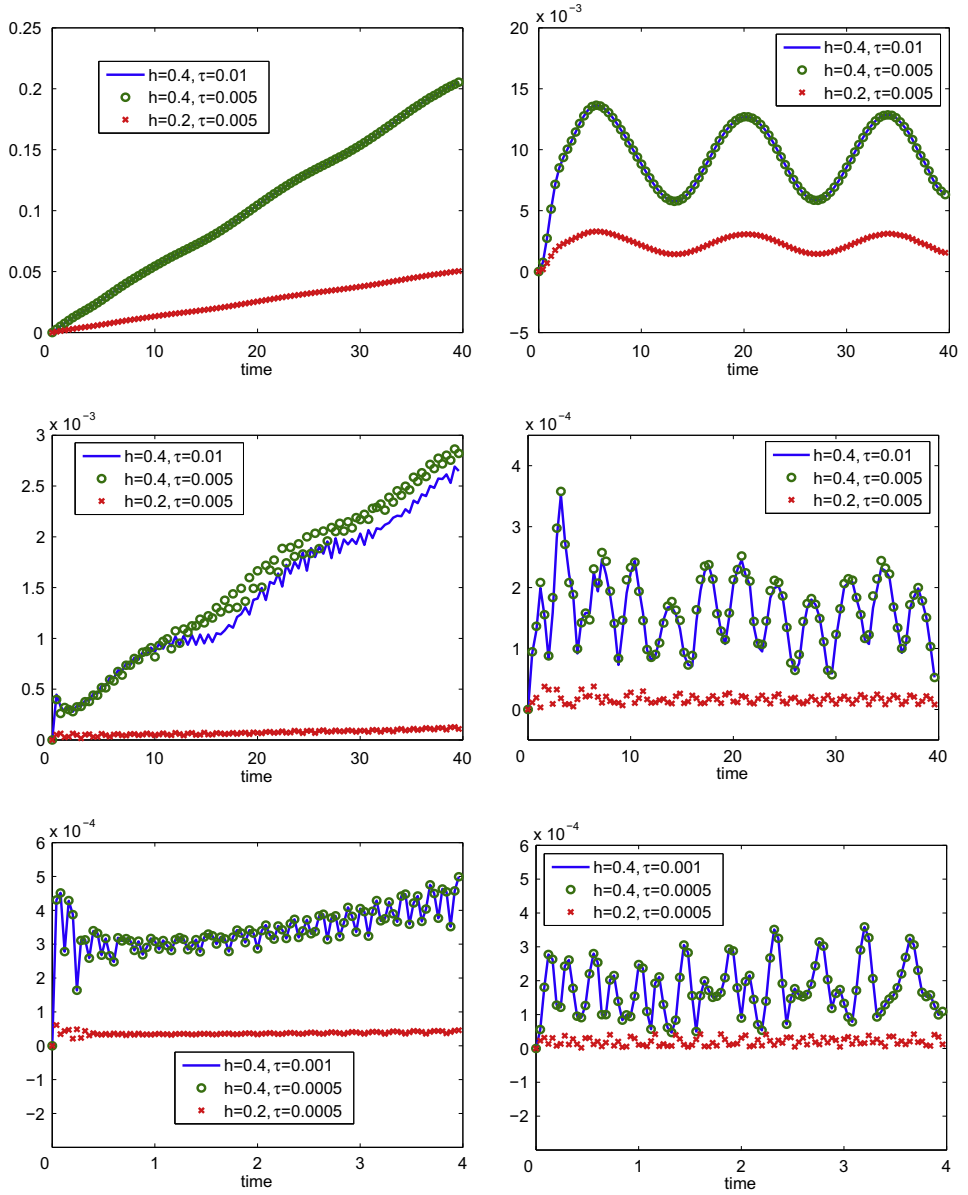

Fig. 5. Maximum solution errors $(\text{error}_\varphi)_l$ (left) and $(\text{error}_u)_l$ (right) with different spatial and temporal stepsizes for scheme $\mathcal{SN}_{42}$ (above), scheme $\mathcal{SN}_{24}$ (middle) and scheme $\mathcal{SN}_{44}$ (below).

$$\begin{array}{c|ccc} 0 & -\frac{1}{12} & \frac{1}{12} & 0 \\ \frac{1}{2} & \frac{5}{48} & \frac{1}{48} & 0 \\ 1 & \frac{1}{6} & \frac{1}{3} & 0 \\ \hline & \frac{1}{6} & \frac{1}{3} & 0 \\ & \frac{1}{6} & \frac{2}{3} & \frac{1}{6} \end{array} \tag{5.7}$$

in the x-direction to both of them. Then, we get another explicit multi-symplectic scheme referred to as $\mathcal{SN}_{24}$, which is high-order in the space direction.

Finally, we combine the temporal discretizations of the scheme $\mathcal{SN}_{42}$ and the spatial approximations of the scheme $\mathcal{SN}_{24}$ to discretize the KGS equations (1.1) correspondingly, a new multi-symplectic method is thus obtained and denoted by $\mathcal{SN}_{44}$, which is high-order both in time and in space. As for the three new constructed schemes, we have the following proposition:

Proposition 5.1. *The numerical schemes $\mathcal{SN}_{42}, \mathcal{SN}_{24}, \mathcal{SN}_{44}$ all are multi-symplectic; Moreover, they preserve the discrete charge conservation laws as follow:*

$$\frac{1}{2}h\sum_k |\varphi_k^{l+1}|^2 + \frac{1}{2}h\sum_k |\varphi_{k+1}^{l+1}|^2 = \frac{1}{2}h\sum_k |\varphi_k^{l}|^2 + \frac{1}{2}h\sum_k |\varphi_{k+1}^{l}|^2,$$

$$\frac{1}{6}h\sum_k |\varphi_k^{l+1}|^2 + \frac{2}{3}h\sum_k |\varphi_{k+\frac{1}{2}}^{l+1}|^2 + \frac{1}{6}h\sum_k |\varphi_{k+1}^{l+1}|^2 = \frac{1}{6}h\sum_k |\varphi_k^{l}|^2 + \frac{2}{3}h\sum_k |\varphi_{k+\frac{1}{2}}^{l+1}|^2 + \frac{1}{6}h\sum_k |\varphi_{k+1}^{l}|^2,$$

$$\frac{1}{6}h\sum_k |\varphi_k^{l+1}|^2 + \frac{2}{3}h\sum_k |\varphi_{k+\frac{1}{2}}^{l+1}|^2 + \frac{1}{6}h\sum_k |\varphi_{k+1}^{l+1}|^2 = \frac{1}{6}h\sum_k |\varphi_k^{l}|^2 + \frac{2}{3}h\sum_k |\varphi_{k+\frac{1}{2}}^{l+1}|^2 + \frac{1}{6}h\sum_k |\varphi_{k+1}^{l}|^2,$$

respectively, provided with zero boundary conditions, i.e. $\varphi_0^l = \varphi_J^l = 0, \forall\ l$.

It can be verified that the truncation error of the scheme $\mathcal{SN}_{42}$ is $\mathcal{O}(h^2+\tau^4)$, $\mathcal{SN}_{24}$ $\mathcal{O}(h^4+\tau^2)$ and the last one $\mathcal{O}(h^4+\tau^4)$, which can also be read from Fig. 5 numerically. As demonstrated the low-order schemes in Section 4, here we also investigate the errors in preserving the conservation laws quantitatively by means of changing the stepsizes as well. The numerical results by the former two schemes are exhibited over time $[0, 40]$. Roughly speaking, high-order explicit numerical methods are not of good stability in general, namely the Courant number [10] should be restricted to very small, it means that the temporal stepsize should be taken very small. The scheme $\mathcal{SN}_{44}$ considered here is of high-order both in the time and in space, for the considerations of the stability and storage, its numerical results are here displayed only over the time interval $[0, 4]$, which seems much shorter than the time for the two schemes $\mathcal{SN}_{42}$ and $\mathcal{SN}_{24}$, but the step number is the same as or more than that by using the former two in the longer time interval $[0, 40]$.

In Fig. 6, we give a list of numerical results of the global errors of charge for these three high-order schemes with different stepsizes upon the conditions that $q = 0, x_0 = 0$. It follows from the numerical results displayed in Fig. 6 that the three high-order schemes all preserve their corresponding discrete analogues of the charge conservation law almost exactly, which is consistent with the theoretical result given in Theorem 3.1.

From the numerical results given from changing processes of stepsizes exhibited in Fig. 7, it can be concluded that the global error of the discrete total energy by the scheme $\mathcal{SN}_{42}$ roughly reaches the magnitude of $\mathcal{O}(\tau^4 h^2)$, the scheme $\mathcal{SN}_{24}$

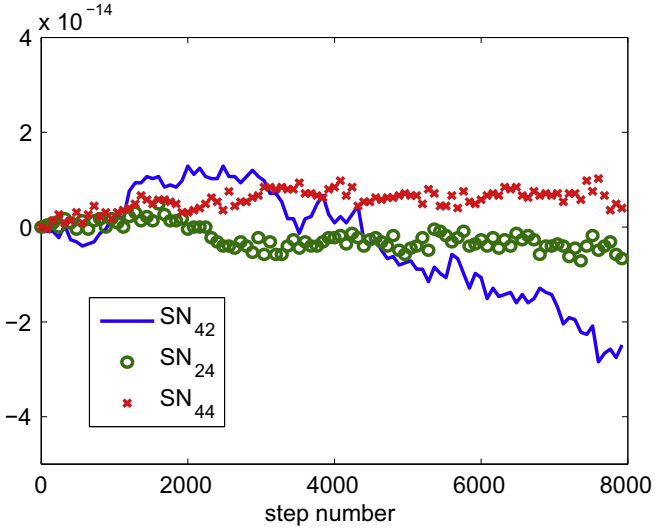

Fig. 6. Global error of charge $(\mathcal{E}_{tc})_l$ for $\mathcal{SN}_{42}$, $\mathcal{SN}_{24}$ with $\tau = 0.005$ and $h = 0.4$; and for $\mathcal{SN}_{44}$ with $\tau = 0.0005$ and $h = 0.4$.

$\mathcal{O}(\tau^2 h^4)$ and the scheme $\mathcal{SN}_{44}\mathcal{O}(\tau^4 h^4)$. The third numerical results presented show that the errors in energy by $\mathcal{SN}_{44}$ are all almost within roundoff, this would not be a surprise that for the three choices of the stepsizes the scales of the order $\mathcal{O}(\tau^4 h^4)$ are in the unit of at least 10^{-13}, almost the roundoff. Moreover, we can't get the exact theoretical predictions of the error decays consistent with the order $\mathcal{O}(\tau^4 h^4)$ in such small scales. From the longitudinal (right) graphs in Fig. 7, it can be read roughly that scheme $\mathcal{SN}_{42}$ preserves the discrete total momentum in the scale of $\mathcal{O}(h^3)$, the scheme $\mathcal{SN}_{24}\mathcal{O}(h^5)$ and the scheme $\mathcal{SN}_{44}$ $\mathcal{O}(h^5)$ too. This indicates that the error of momentum is related to the spatial mesh grid size h only. Based on the numerical results presented in Section 4 and Appendix, we give the following two conjectures

(1) The multi-symplectic scheme (3.3)–(3.18) can preserve the discrete total energy in the order of $\mathcal{O}(h^p \tau^q)$, where p and q are the orders of the methods applied to the spatial direction and the temporal direction, respectively.
(2) The error in preserving the discrete momentum is of order $\mathcal{O}(h^{p+1})$.

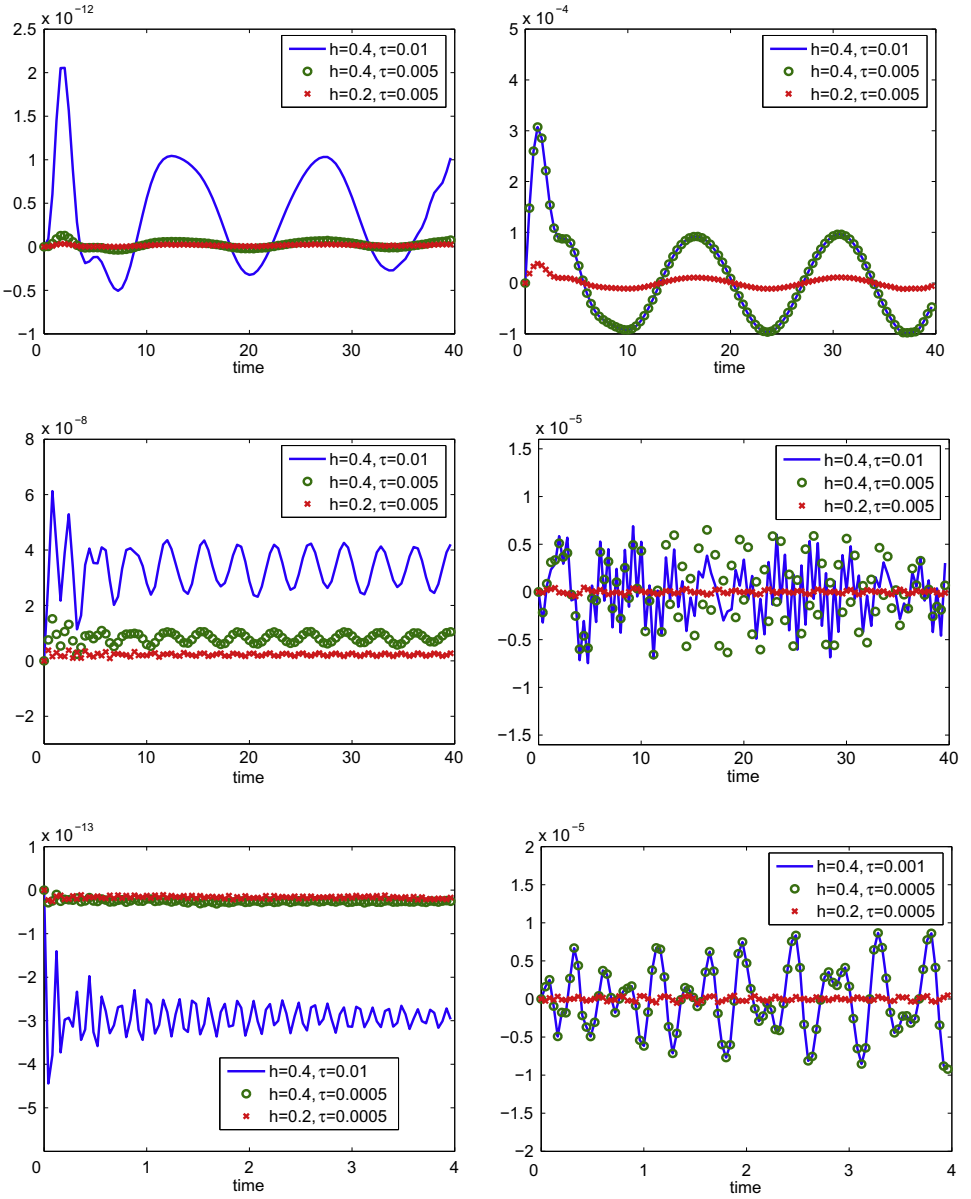

Fig. 7. Global errors of the energy and momentum, i.e., $(\mathcal{E}_{te})_l$ (left) and $(\mathcal{E}_{tm})_l$ (right) for scheme $\mathcal{SN}_{42}$ (above), scheme $\mathcal{SN}_{24}$ (middle) and scheme $\mathcal{SN}_{44}$ (below) with different spatial and temporal stepsizes.

References

[1] U.M. Ascher, R.I. Mclanchlan, Multisymplectic box schemes and the Korteweg–de Vries equation, Appl. Numer. Math. 48 (2004) 255–269.
[2] W. Bao, L. Yang, Efficient and accurate numerical methods for the Klein–Gordon–Schrödinger equations, J. Comput. Phys. 225 (2007) 1863–1893.
[3] T.J. Bridges, S. Reich, Multi-symplectic integrators: numerical schemes for Hamiltonian PDEs that conserve symplecticity, Phys. Lett. A 284 (2001) 184–193.
[4] T.J. Bridges, S. Reich, Multi-symplectic spectral discretizations for the Zakharove–Kuznetsov and shallow-water equations, Physica D 152 (2001) 491–504.
[5] T.J. Bridges, S. Reich, Numerical methods for Hamiltonian PDEs, J. Phys. A: Math. Gen. 39 (2006) 5287–5320.
[6] J. Hong, S. Jiang, C. Li, H. Liu, Explicit multi-symplectic methods for Hamiltonian wave equations, Commun. Comput. Phys. 2 (4) (2007) 662–683.
[7] J. Hong, C. Li, Multi-symplectic Runge–Kutta methods for nonlinear Dirac equations, J. Comput. Phys. 211 (2006) 448–472.
[8] J. Hong, X. Liu, C. Li, Multi-symplectic Runge–Kutta–Nyström methods for nonlinear Schrödinger equations with variable coefficients, J. Comput. Phys. 226 (2007) 1968–1984.
[9] J. Hong, Y. Liu, H. Munthe-Kaas, A. Zanna, Globally conservative properties and error estimation of a multi-symplectic scheme for Schrödinger equations with variable coefficients, Appl. Numer. Math. 56 (2006) 814–843.
[10] A. Iserles, A First Course in the Numerical Analysis of Differential Equations, Cambridge University Press, Cambridge, 1996.
[11] A.L. Islas, C.M. Schober, On the preservation of phase space structure under multisymplectic discretization, J. Comput. Phys. 197 (2004) 585–609.
[12] L. Kong, R. Liu, Z. Xu, Numerical simulation of interaction between Schrödinger field and Klein–Gordon field by multisymplectic method, Appl. Math. Comput. 81 (2006) 342–350.
[13] D. Okumbor, R.D. Skeel, Explicit canonical methods for Hamiltonian systems, Math. Comput. 59 (200) (1992) 439–455.
[14] S. Reich, Multi-symplectic Runge–Kutta collocation methods for Hamiltonian wave equation, J. Comput. Phys. 157 (2000) 473–499.
[15] J.M. Sanz-Serna, M.P. Calvo, Numerical Hamiltonian Problems, Chapman & Hall, London, 1994.
[16] Y. Wang, B. Wang, High-order multi-symplectic schemes for the nonlinear Klein–Gordon equation, Appl. Math. Comput. 166 (2005) 608–632.
[17] X. Xiang, Spectral method for solving the system of equations of Schrödinger–Klein–Gordon field, J. Comput. Appl. Math 21 (1988) 161–171.
[18] L. Zhang, Convergence of a conservative difference scheme for a class of Klein–Gordon–Schrödinger equations in one space dimension, Appl. Math. Comput. 163 (2005) 343–355.